Growth of Graphene from Food, Insects, and Waste

Gedeng Ruan,[†,⊥] Zhengzong Sun,[†,⊥] Zhiwei Peng,[†] and James M. Tour[†,‡,§,*]

[†]Department of Chemistry, [‡]Department of Mechanical Engineering and Materials Science, and [§]Richard E. Smalley Institute for Nanoscale Science and Technology, Rice University, 6100 Main Street, Houston, Texas 77005, United States. [⊥]These authors contributed equally to this work.

ABSTRACT In its monolayer form, graphene is a one-atom-thick two-dimensional material with excellent electrical, mechanical, and thermal properties. Large-scale production of high-quality graphene is attracting an increasing amount of attention. Chemical vapor and solid deposition methods have been developed to grow graphene from organic gases or solid carbon sources. Most of the carbon sources used were purified chemicals that could be expensive for mass production. In this work, we have developed a less expensive approach using six easily obtained, low or negatively valued raw carbon-containing materials used without prepurification (cookies, chocolate, grass, plastics, roaches, and dog feces) to grow graphene directly on the backside of a Cu foil at 1050 °C under H_2/Ar flow. The nonvolatile pyrolyzed species were easily removed by etching away the frontside of the Cu. Analysis by Raman spectroscopy, X-ray photoelectron spectroscopy, ultraviolet–visible spectroscopy, and transmission electron microscopy indicates that the monolayer graphene derived from these carbon sources is of high quality.

KEYWORDS: monolayer graphene · CVD growth · inexpensive carbon sources

Graphene, in its monolayer form, is an attractive two-dimensional material with an atomically thick honeycomb structure.[1−3] Due to its extraordinary electrical,[4] mechanical,[5] thermal,[6] and spintronic[7] properties, graphene has the potential to be applied in nanoelectronic devices[8,9] and in nanocomposites.[10,11] In the past years, many methods for production of graphene, such as exfoliation, chemical methods, and chemical vapor deposition (CVD), have appeared in the literature. For the exfoliation methods, researchers originally used adhesive tape to mechanically peel away the graphite crystals into few-layer or monolayer graphene.[1,4] Later, liquid exfoliation methods[12−14] were reported, consisting of chemical oxidation and dispersion of graphite, reduction of graphite oxide, and annealing in Ar/H_2. Although it could become an industrially important method to produce graphene,[15] until now the quality of this liquid exfoliated graphene is still lower than mechanically exfoliated graphene due to the destruction of the basal plane structure during the oxidation and incomplete removal of the functional groups. Recently, many research groups have published several CVD methods for growing large-sized graphene on wafers. For the growth of epitaxial graphene on single-crystal silicon carbide (SiC),[16,17] the cost of this graphene is high due to the price of the 4H-SiC substrate. Also, metals such as copper,[18] nickel,[19,20] iron,[21] cobalt,[22] and platinum[23] have been used as catalytic substrates to grow mono-, bi-, or multilayer graphene. The carbon source can be a gas, such as methane or acetylene, or solid carbon sources, such as poly(methyl methacrylate) (PMMA) or sucrose.[24] However, all of these are purified chemicals.

Here we demonstrate that much less expensive carbon sources, such as food, insects, and waste, can be used without purification to grow high-quality monolayer graphene directly on the backside of Cu foils under the H_2/Ar flow. For food, a Girl Scout cookie and chocolate were investigated. For waste with low or negative monetary value, we used bulk polystyrene plastic, a common solid waste, blades of grass, and dog feces. For insects, another often negative value carbon source, a cockroach leg, was used. Growing high-quality graphene from these carbon sources opens a new way to convert the waste carbon into a high-value-added product, as graphene is one of the most expensive materials in the world.[25] We propose a possible purification and growth mechanism. The graphene forms as the solid carbon sources decompose and diffuse to the backside of the Cu foil, leaving the other elemental residues on the original side. Using this procedure, only high-quality pristine graphene with few defects and ~97% transparency was grown on the backside of the Cu foil, as confirmed by Raman and UV–vis spectroscopy. No heteroatoms were detected in the monolayer graphene according to X-ray photoelectron spectroscopy (XPS), suggesting its pristine nature. Analysis by selected area diffraction pattern (SAED) in transmission electron microscopy

* Address correspondence to tour@rice.edu.

Received for review July 13, 2011 and accepted July 29, 2011.

Published online July 29, 2011
10.1021/nn202625c

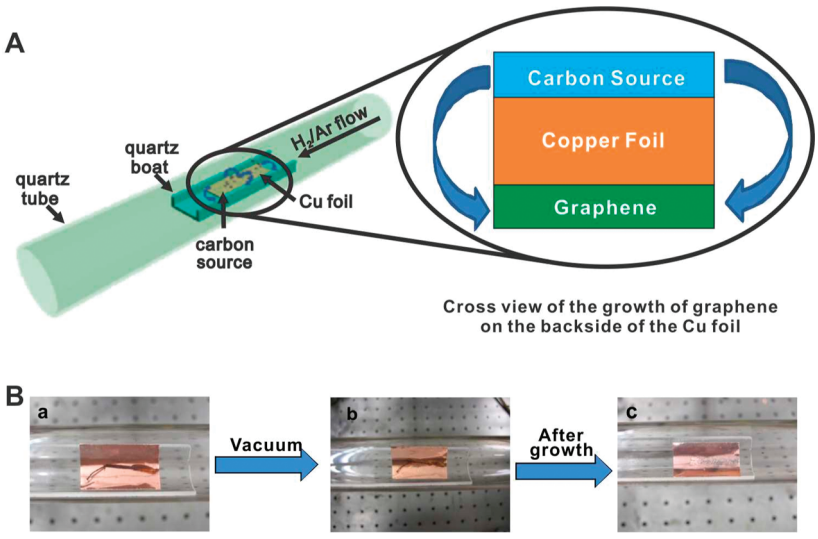

Figure 1. (A) Diagram of the experimental apparatus for the growth of graphene from food, insects, or waste in a tube furnace. On the left, the Cu foil with the carbon source contained in a quartz boat is placed at the hot zone of a tube furnace. The growth is performed at 1050 °C under low pressure with a H_2/Ar gas flow. On the right is a cross view that represents the formation of pristine graphene on the backside of the Cu substrate. (B) Growth of graphene from a cockroach leg. (a) One roach leg on top of the Cu foil. (b) Roach leg under vacuum. (c) Residue from the roach leg after annealing at 1050 °C for 15 min. The pristine graphene grew on the bottom side of the Cu film (not shown).

(TEM) confirms the hexagonal lattice structure of the graphene.

RESULTS AND DISCUSSION

In a typical growth experiment, as shown in Figure 1A, 10 mg of the dry carbon source was placed atop a Cu foil, and the foil was introduced into a 1050 °C tube furnace. The sample was annealed for 15 min under low pressure with H_2 and Ar at a flow rate of 100 and 500 cm^3 STP min^{-1}, respectively. For the grass and dog feces, the samples were heated in a 65 °C vacuum (102 Torr) oven for 10 h to remove excess moisture. The experimental setup and procedures are similar to the method used to grow PMMA-derived graphene.[24] The main difference in this work is that the high-quality monolayer graphene only forms on the backside of the Cu foil, while the PMMA-derived graphene grows on both sides of the Cu foil.

Since the carbon sources contain non-carbon elements, nonvolatile residue may remain on the Cu foil after annealing. Supporting Information Figure S1 shows SEM images of both sides of the Cu foil after a growth experiment. On the original frontside, many residual particles were found, as shown in Figure S1A, while almost no particles were observed on the backside of the Cu foil where the graphene is formed (Figure S1B). In Figure 1B, photographic images of different growth stages are shown and black residue is present after the growth in Figure 1Bc. On the basis of the experimental evidence during the growth, most of the carbon segments from the decomposition of the solids are carried away as gases by the H_2/Ar flow. However, since the quartz boat has a semicircular shape, the slightly bent Cu foil is supported by the quartz boat and a portion of the carbon source diffused to the backside of the Cu foil, forming a monolayer graphene film. It is not known whether the diffusion is through the Cu foil or *via* the edges. As a comparison experiment, if the solid carbon sources were placed 5 cm ahead of the Cu substrate (but still in the quartz boat) and both were introduced into the hot furnace at the same time, only amorphous carbon formed on both sides of the Cu foil; the representive Raman spectrum of the film displays a large D peak as shown in Supporting Information Figure S2.

After the monolayer graphene samples on the backside of the Cu foil were transferred onto a 100 nm SiO_2/Si wafer using standard protocols,[24] the product was analyzed using Raman spectroscopy at 514 nm laser excitation. As shown in Figure 2, all of the graphene samples grown have small or no D peaks in their Raman spectra, an indication of few graphene defects.[26] The large 2D/G ratio suggests that it is high-quality monolayer graphene. The exact G and 2D peak positions and their full width at half-maximum (fwhm) for each spectrum were measured and are summarized in Supporting Information Table S1; the results are similar to previously reported graphene data.[27] The G and 2D peaks are located at 1585.5−1591.4 and 2682.6−2693.9 cm^{-1}, respectively. The fwhm values of the G peak and 2D peak are 14.1−16.3 and 32.0−35.1 cm^{-1}, respectively. In order to investigate the uniformity of the graphene film, a Raman mapping over a 100 × 100 μm^2 area (graphene derived from dog feces) was acquired. Over 95% of the

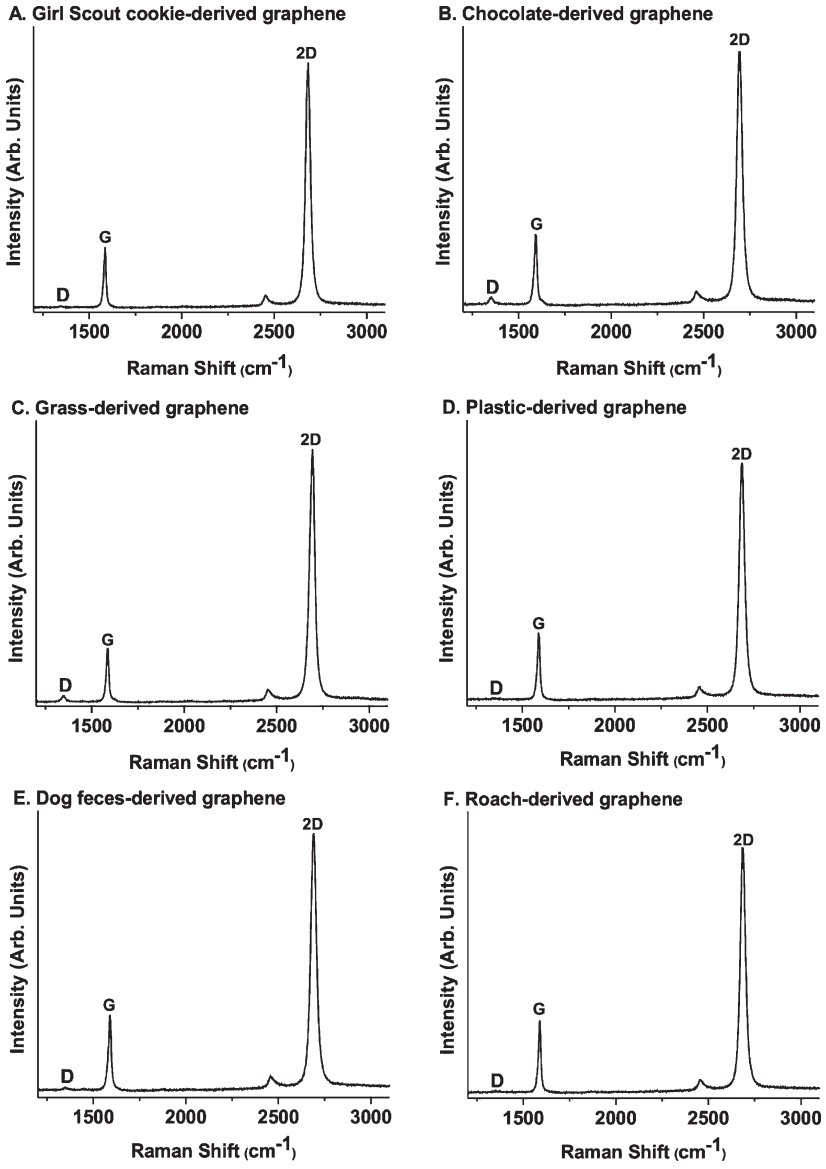

Figure 2. Raman spectra of monolayer graphene from six different carbon sources. The Raman spectra graphene were derived from (A) Girl Scout cookie; (B) chocolate; (C) grass; (D) plastic (polystyrene Petri dish); (E) dog feces, and (F) a cockroach leg. There was only a trace D peak in some of the spectra, and the 2D to G peak intensity ratios were ~4, indicating monolayer graphene.

scanned area had a signature of $I_{2D}/I_G > 1.8$ and $I_D/I_G < 0.1$, which further demonstrated the high quality of the monolayer graphene, as shown in Supporting Information Figure S3.

XPS analysis of the graphene films was performed to confirm the elemental composition and the chemical environment of the C atoms. In Figure 3, only a sharp peak at 284.5 eV with an asymmetric tailing toward high bonding energy is observed for the C1s peak, suggesting a sp^2 graphitic peak.[28−30] The fwhm was ~1.1 eV for each C1s peak. Although the raw carbon sources contain other elements such as oxygen, nitrogen, iron, sulfur, or phosphorus, the obtained graphene consisted of carbon, with none of these other elements found in the XPS survey spectra, confirming the graphene's pristine composition.

In the growth system, the H_2 gas might act as both a reducing reagent and a carrier gas. Since carbon is the most abundant element in these materials and graphene is the most thermodynamically stable form of carbon,[31] only pristine graphene forms on the Cu. According to the C−C bond length (0.142 nm) in the hexagonal lattice of graphene,[32] the surface area of one side of a monolayer of graphene is about 1315 m^2/g.[33] Theoretically, it only takes 228 ng of carbon to cover one side of a 2 cm × 3 cm Cu foil with monolayer graphene. In our growth system, the size of the graphene is ultimately limited by the size of the tube furnace, which limits the size of the Cu substrate

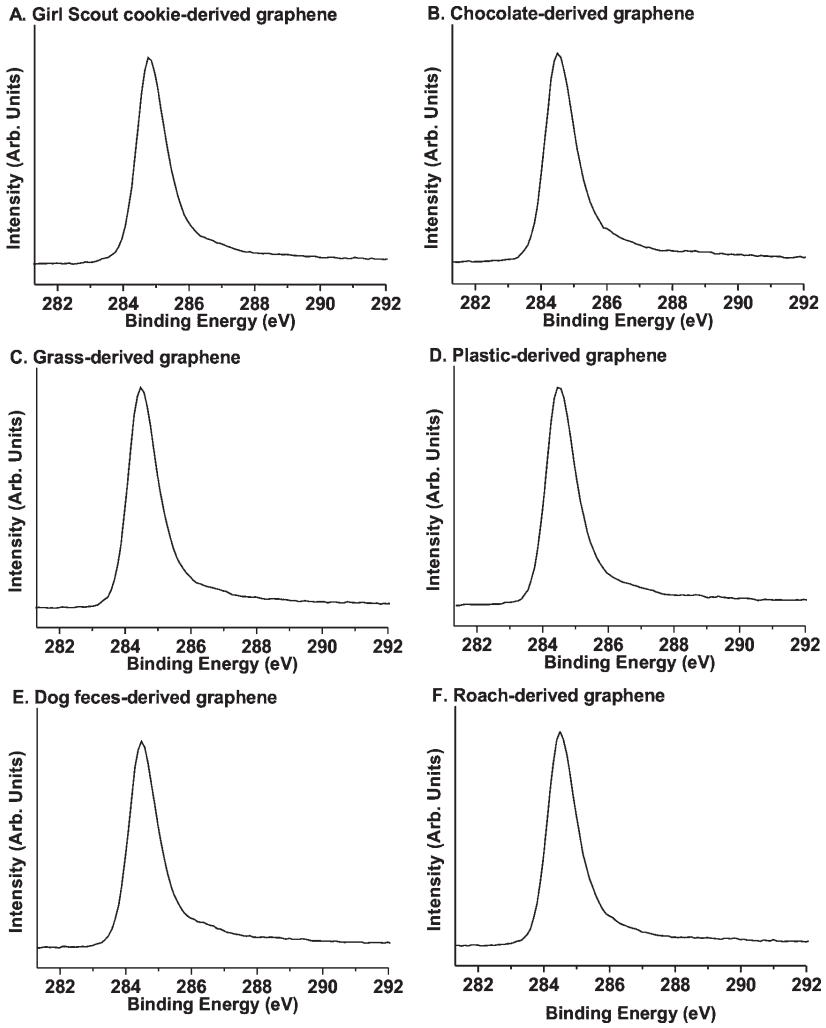

Figure 3. XPS spectra of graphene from six carbon sources. The C1s XPS spectra of the randomly selected detection spots on graphene derived from the various sources.

that can be used. With a larger furnace, larger-sized graphene could be produced with 10 mg of the carbon source. Therefore, the limiting reagent in this work is the Cu foil, though scrolled Cu foil could provide enhanced surface areas.

All of the graphene films were transferred to a quartz slides before UV−vis analysis. In the spectra, each graphene film exhibits a peak at 268 nm, a typical $\pi \rightarrow \pi^*$ transition for the aromatic C−C bond in graphene,[34,35] and the typical (2.4 ± 0.1%) absorption at 550 nm corresponding to the monolayer nature of graphene,[24,36] as shown in Figure 4. In the photographic images, the graphene films on quartz slides are unifom and transparent. Also, the sheet resistance (R_s) of the graphene was in the range of 1.5−3.0 kΩ/square by the four-probe method.

TEM images and the selected area electron diffraction (SAED) pattern were taken to determine the crystal structure of a representative graphene sample derived from the cookie. The graphene was transferred to a c-flat TEM grid (Protochips), where most of the area of the graphene was determined to be crystalline by its hexagonal diffraction pattern (Figure 5A) and was continuous as shown in Figure 5B. A randomly chosen monolayer edge of the graphene was imaged in Figure 5C. The edge of the graphene corresponds to monolayer graphene, corroborating the UV−vis spectra and Raman data. The dark spots in the image in Figure 5C might arise from the PMMA residues introduced during the etching and transferring step.[24]

CONCLUSION

We have demonstrated a general method to grow high-quality graphene from various raw carbon materials at 1050 °C under vacuum and H_2/Ar flow. The carbon sources were foods (cookie and chocolate), waste (grass, plastic, dog feces) and insect-derived. With this technique, many kinds of solid materials that contain carbon can potentially

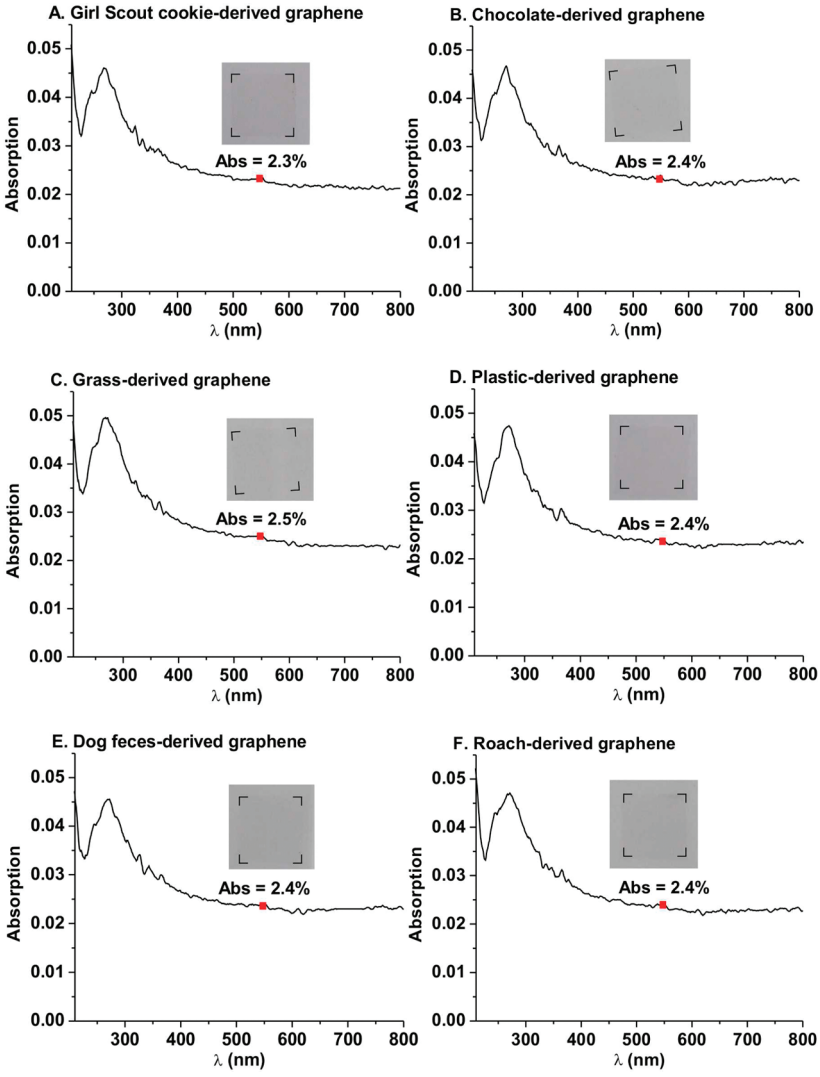

Figure 4. UV−vis spectra of graphene derived from six carbon sources. The absorbance of each monolayer graphene film at 550 nm is approximately 2.4 ± 0.1%. On the right top of each spectrum is the photographic image of the monolayer graphene film of ~1 cm × 1 cm in size on a 1 mm thick quartz slide; the graphene is labeled with a dashed square.

be used without purification as the feedstocks to produce high-quality graphene. Furthermore, through this method, low-valued foods and negative-valued solid wastes are successfully transformed into high-valued graphene which brings new solutions for recycling of carbon from impure sources.

EXPERIMENTAL METHODS

Growth and Transfer of Graphene Samples. Six different carbon sources were used: Girl Scout cookie (the Girl Scouts of America Troop 25080 from Houston, Texas, provided the cookies, shortbread flavor), chocolate (Chocolate Kennedy Half Dollar Gold Coins), grass (Ophiopogon picked at Rice University), plastic (Fisherbrand polystyrene Petri dishes, catalog #08-757-12), dog feces (Miniature Dachsund), and a cockroach leg (American cockroach caught in a house). The grass and the dog feces were dehydrated in a vacuum oven (102 Torr) at 65 °C for 10 h before being used in the growth process.

The CVD system was evacuated to 10 mTorr for 10 h before growth. For the growth of graphene, 10 mg of a carbon source was placed atop the Cu foil (99.8% purity). The Cu foil was slightly bent to better retain the solid sources without spilling. The foil was then supported by the steeper-curved quartz boat, as shown in Figure 6. The sample was annealed at 1050 °C for 15 min with Ar flow at 500 cm^3 STP min^{-1} and H_2 flow at 100 cm^3 STP min^{-1}. The pressure was 9.3 Torr during growth. When growing graphene from different carbon sources, the quartz tube and boat were cleaned by annealing them at 1050 °C in air for 10 min between each growth to eliminate cross contamination. The system was then fast cooled (moved to the cool zone using a magnetic transfer rod) to room temperature under the H_2/Ar flow. A 100 nm thick PMMA film was deposited on the backside of the foil using a 4% PMMA anisole solution spin-coated at 3000 rpm for 40 s. The frontside of the Cu foil was etched away by floating the foil metal-down on an acidic $CuSO_4$ solution (made with $CuSO_4 \cdot 5H_2O$ (15.6 g), conc. HCl (50 mL), H_2O (50 mL), and H_2SO_4 (2 mL)) for ~5 s, then dipping the foil in DI water; this process was repeated at least two times in order to wash away the residue left on the frontside of the Cu foil. If the water washes did not remove the residue from the frontside of the Cu foil, a Kimwipe was used to

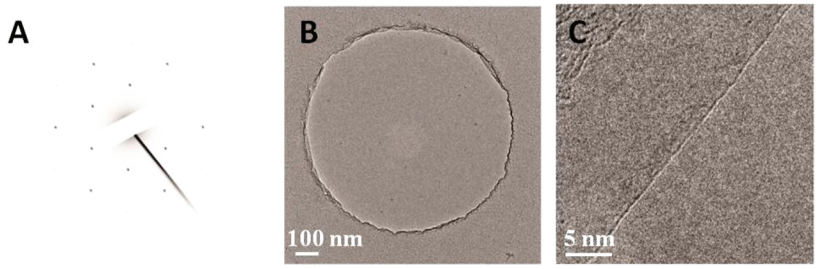

Figure 5. Diffraction pattern and TEM images of the cookie-derived graphene. (A) SAED pattern, (B) suspended graphene film on a 1 μm diameter hole, and (C) the edge of monolayer graphene.

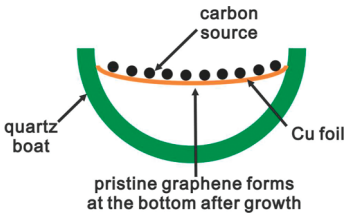

Figure 6. Arrangement of the Cu foil within the quartz boat. The size of the Cu foil was ~2 cm × 3.0 cm and the boat was 40 cm long and cut from a quartz tube with a 15 mm inside diameter.

carefully brush the residue away before all of the Cu was removed. The PMMA-coated graphene was transferred to different substrates such as 100 nm SiO_2/Si wafers and quartz. After the film was completely dried in a vacuum oven at 65 °C for 2 h, the film was rinsed with acetone three times before characterization.

Characterization. Raman spectra were obtained by the single scan generated by the WiRE spectral acquisition wizard using a 514.5 nm laser in a Renishaw Raman RE02 microscope. UV−vis spectroscopy was done using a 1 mm thick quartz slide on which the sample was placed in a Shimadzu UV-3101 system. The XPS spectra were obtained using a 100 μm X-ray beam of the 45° takeoff angle and 26.00 eV pass energy in a PHI Quantera SXM scanning X-ray microprobe system. TEM imaging was obtained in a 2100F field emission gun transmission electron microscope. The graphene samples were transferred to a c-flat TEM grid (Protochips).

Acknowledgment. This work was funded by Sandia National Laboratory (1100745), the Air Force Office of Scientific Research (FA9550-09-1-0581), and the ONR MURI program (00006766, N00014-09-1-1066).

Supporting Information Available: SEM images, Raman spectra, Table S1. This material is available free of charge *via* the Internet at http://pubs.acs.org.

REFERENCES AND NOTES

1. Novoselov, K. S.; Geim, A. K.; Morozov, S. V.; Jiang, D.; Zhang, Y.; Dubonos, S. V.; Grigorieva, I. V.; Firsov, A. A. Electric Field Effect in Atomically Thin Carbon Films. *Science* **2004**, *306*, 666–669.
2. Novoselov, K. S.; Geim, A. K.; Morozov, S. V.; Jiang, D.; Katsnelson, M. I.; Grigorieva, I. V.; Dubonos, S. V.; Firsov, A. A. Two-Dimensional Gas of Massless Dirac Fermions in Graphene. *Nature* **2005**, *438*, 197–200.
3. Geim, A. K.; Novoselov, K. The Rise of Graphene. *Nat. Mater.* **2007**, *6*, 183–191.
4. Chen, J. H.; Jang, C.; Xiao, S.; Ishigami, M.; Fuhrer, M. S. Intrinsic and Extrinsic Performance Limits of Graphene Devices on SiO_2. *Nat. Nanotechnol.* **2008**, *3*, 206–209.
5. Lee, C.; Wei, X.; Kysar, J. W.; Hone, J. Measurement of the Elastic Properties and Intrinsic Strength of Monolayer Graphene. *Science* **2008**, *321*, 385–388.
6. Balandin, A. A.; Ghosh, S.; Bao, W.; Calizo, I.; Teweldebrhan, D.; Miao, F.; Lau, C. N. Superior Thermal Conductivity of Single-Layer Graphene. *Nano Lett.* **2008**, *8*, 902–907.
7. Wang, W. L.; Meng, S.; Kaxiras, E. Graphene Nanoflakes with Large Spin. *Nano Lett.* **2008**, *8*, 241–245.
8. Schwierz, F. Graphene Transistors. *Nat. Nanotechnol.* **2010**, *5*, 487–496.
9. Lin, Y. M.; Dimitrakopoulos, C.; Jenkins, K. A.; Farmer, D. B.; Chiu, H. Y.; Grill, A.; Avouris, P. 100-GHz Transistors from Wafer-Scale Epitaxial Graphene. *Science* **2010**, *327*, 662.
10. Ramanathan, T.; Abdala, A. A.; Stankovich, S.; Dikin, D. A.; Herrera-Alonso, M.; Piner, R. D.; Adamson, D. H.; Schniepp, H. C.; Chen, X.; Ruoff, R. S.; *et al.* Functionalized Graphene Sheets for Polymer Nanocomposites. *Nat. Nanotechnol.* **2008**, *3*, 327–331.
11. Kim, H.; Abdala, A. A.; Macosko, C. W. Graphene/Polymer Nanocomposites. *Macromolecules* **2010**, *43*, 6515–6530.
12. Hernandez, Y.; Nicolosi, V.; Lotya, M.; Blighe, F. M.; Sun, Z.; De, S.; McGovern, I. T.; Holland, B.; Byrne, M.; Gun'Ko, Y. K.; *et al.* High-Yield Production of Graphene by Liquid-Phase Exfoliation of Graphite. *Nat. Nanotechnol.* **2008**, *3*, 563–568.
13. Stankovich, S.; Dikin, D. A.; Piner, R. D.; Kohlhaas, K. A.; Kleinhammes, A.; Jia, Y.; Wu, Y.; Nguyen, S. T.; Ruoff, R. S. Synthesis of Graphene-Based Nanosheets *via* Chemical Reduction of Exfoliated Graphite Oxide. *Carbon* **2007**, *45*, 1558–1565.
14. Marcano, D. C.; Kosynkin, D. V.; Berlin, J. M.; Sinitskii, A.; Sun, Z.; Slesarev, A.; Alemany, L. B.; Lu, W.; Tour, J. M. Improved Synthesis of Graphene Oxide. *ACS Nano* **2010**, *4*, 4806–4814.
15. Segal, M. Selling Graphene by the Ton. *Nat. Nanotechnol.* **2009**, *4*, 612–614.
16. Berger, C.; Song, Z.; Li, X.; Wu, X.; Brown, N.; Naud, C.; Mayou, D.; Li, T.; Hass, J.; Marchenkov, A. N.; *et al.* Electronic Confinement and Coherence in Patterned Epitaxial Graphene. *Science* **2006**, *312*, 1191–1196.
17. Berger, C.; Song, Z.; Li, T.; Li, X.; Ogbazghi, A. Y.; Rui, F.; Dai, Z.; Marchenkov, A. N.; Conrad, E. H.; Phillip, N.; *et al.* Ultrathin Epitaxial Graphite: 2D Electron Gas Properties and a Route toward Graphene-Based Nanoelectronics. *J. Phys. Chem. B* **2004**, *108*, 19912–19916.
18. Li, X.; Cai, W.; An, J.; Kim, S.; Nah, J.; Yang, D.; Piner, R.; Velamakanni, A.; Jung, I.; Tutuc, E.; *et al.* Large-Area Synthesis of High-Quality and Uniform Graphene Films on Copper Foils. *Science* **2009**, *324*, 1312–1314.
19. Reina, A.; Jia, X.; Ho, J.; Nezich, D.; Son, H.; Bulovic, V.; Dresselhaus, M. S.; Kong, J. Large Area, Few-Layer Graphene Films on Arbitrary Substrates by Chemical Vapor Deposition. *Nano Lett.* **2009**, *9*, 30–35.
20. Kim, K. S.; Zhao, Y.; Jang, H.; Lee, S. Y.; Kim, J. M.; Kim, K. S.; Ahn, J. H.; Kim, P.; Choi, J. Y.; Hong, B. H. Large-Scale Pattern Growth of Graphene Films for Stretchable Transparent Electrodes. *Nature* **2009**, *457*, 706–710.
21. Kondo, D.; Sato, S.; Yagi, K.; Harada, N.; Sato, M.; Nihei, M.; Yokoyama, N. Low-Temperature Synthesis of Graphene and Fabrication of Top-Gated Field Effect Transistors without Using Transfer Processes. *Appl. Phys. Express* **2010**, *3*, 025102.
22. Ago, H.; Ito, Y.; Mizuta, N.; Yoshida, K.; Hu, B.; Orofeo, C. M.; Tsuji, M.; Ikeda, K.; Mizuno, S. Epitaxial Chemical Vapor

Deposition Growth of Single-Layer Graphene over Cobalt Film Crystallized on Sapphire. *ACS Nano* **2010**, *4*, 7407–7414.
23. Kang, B. J.; Mun, J. H.; Hwang, C. Y.; Cho, B. J. Monolayer Graphene Growth on Sputtered Thin Film Platinum. *J. Appl. Phys.* **2009**, *106*, 104309.
24. Sun, Z.; Yan, Z.; Yao, J.; Beitler, E.; Zhu, Y.; Tour, J. M. Growth of Graphene from Solid Carbon Sources. *Nature* **2010**, *468*, 549–552.
25. Geim, A. K.; Kim, P. Carbon Wonderland. *Sci. Am.* **2008**, *298*, 90–97.
26. Ferrari, A. C.; Meyer, J. C.; Scardaci, V.; Casiraghi, C.; Lazzeri, M.; Mauri, F.; Piscanec, S.; Jiang, D.; Novoselov, K. S.; Roth, S.; *et al.* Raman Spectrum of Graphene and Graphene Layers. *Phys. Rev. Lett.* **2006**, *97*, 18740.
27. Wang, Y. Y.; Ni, Z. H.; Yu, T.; Shen, Z. X.; Wang, H. M.; Wu, Y. H.; Chen, W.; Wee, A. T. S. Raman Studies of Monolayer Graphene: The Substrate Effect. *J. Phys. Chem. C* **2008**, *112*, 10637–10640.
28. Yumitori, S. Correlation of C1s Chemical State Intensities with the O1s Intensity in the XPS Analysis of Anodically Oxidized Glass-like Carbon Samples. *J. Mater. Sci.* **2000**, *35*, 139–146.
29. Evans, S.; Thomas, J. M. The Chemical Nature of Ion-Bombarded Carbon: A Photoelectron Spectroscopic Study of `Cleaned' Surfaces of Diamond and Graphite. *Proc. R. Soc. London, Ser. A* **1977**, *353*, 103–120.
30. Kozlowski, C.; Sherwood, P. M. A. X-ray Photoelectron Spectroscopic Studies of Carbon-Fibre Surfaces. Part 4. The Effect of Electrochemical Treatment in Nitric Acid. *J. Chem. Soc., Faraday Trans. 1* **1984**, *80*, 2099–2107.
31. Gilje, S.; Han, S.; Wang, M.; Wang, K. L.; Kaner, R. B. A Chemical Route to Graphene for Device Applications. *Nano Lett.* **2007**, *7*, 3394–3398.
32. Heyrovska, R. Atomic Structures of Graphene, Benzene and Methane with Bond Lengths as Sums of the Single, Double and Resonance Bond Radii of Carbon. *arXiv.org Physics* **2008**, DOI: arxiv.org/abs/0804.4086.
33. Stoller, M. D.; Park, S. J.; Zhu, Y. W.; An, J. H.; Ruoff, R. S. Graphene-Based Ultracapacitors. *Nano Lett.* **2008**, *8*, 3498–3502.
34. Li, D.; Müller, M. B.; Gilje, S.; Kaner, R. B.; Wallace, G. G. Processable Aqueous Dispersions of Graphene Nanosheets. *Nat. Nanotechnol.* **2008**, *3*, 101–105.
35. Feng, M.; Zhan, H.; Chen, Y. Nonlinear Optical and Optical Limiting Properties of Graphene Families. *Appl. Phys. Lett.* **2010**, *96*, 033107.
36. Nair, R. R.; Blake, P.; Grigorenko, A. N.; Novoselov, K. S.; Booth, T. J.; Stauber, T.; Peres, N. M.; Geim, A. K. Fine Structure Constant Defines Visual Transparency of Graphene. *Science* **2008**, *320*, 1308–1308.